Available online at www.sciencedirect.com
SCIENCE DIRECT®

NUCLEAR SCIENCE AND TECHNIQUES

Nuclear Science and Techniques, Vol.17, No.2 (2006) 78–82

Structure and tribological properties of Ti-containing amorphous carbon coatings prepared by cathode arc-enhanced middle-frequency magnetron sputtering

YANG Bing HUANG Zhi-Hong FAN Xiang-Jun FU De-Jun*

(Accelerator Laboratory, School of Physics, Wuhan University, Wuhan 430072, China)

Abstract Ti-containing amorphous carbon (Ti-aC) coatings were deposited on cemented carbide and Si substrates by cathode-arc-enhanced closed field middle-frequency unbalanced magnetron sputtering. The coatings were studied by using atomic force microscopy, Raman scattering, nanoindentation, and pin-on-disk testing. The measurements showed that the hardness of the coatings increased from 12 GPa at a Ti content of 1 at.% to 27 GPa at 31 at.%. The coatings exhibited different friction behaviors when facing different mating materials and changed with increasing Ti content. The coating with 4 at.% Ti exhibited excellent tribological performance with a low friction coefficient of 0.07 when facing the cemented carbide.

Key words Arc-enhanced magnetron sputtering, Diamond-like carbon, Hardness, Tribological performance

CLC number O484.4

1 Introduction

Much attention has been paid to carbon-based coatings because of their excellent physical and chemical properties, such as low friction coefficient, high wear- and corrosion-resistance and chemical stability. In all, the carbon-based coatings, metal-containing amorphous carbon (Me-aC) has been intensively investigated for many years, since they have excellent mechanical and tribological properties [1-6].

Raman spectroscopy is one of the best ways to obtain the detailed bonding structure of the carbon-based coatings. It has been demonstrated that the intensity ratio between D (disorder) and G (graphite) peaks (I_D/I_G) is qualitatively related to the size of sp^2 clusters and the stress of the coatings. However, little attention has been paid to the influence of bias voltages and doping metal content on the performance of the coatings, especially the relationship between the structure and tribological properties. In this paper, we investigate the structure and tribological properties of the Ti-aC coatings prepared by using an arc-assisted middle-frequency (MF) magnetron sputter system.

2 Experiments details

Ti-aC nanocomposite coatings were deposited by using a homemade industrial-scale cathode arc-enhanced closed field middle-frequency unbalanced magnetron sputter system. The base pressure prior to coating deposition was 7×10^{-4} Pa. During deposition, the substrates rotated in the deposition chamber and faced one pair of Ti targets (99.99%) and three pairs of C targets (99.99%) sequentially. The pulsed bias to the substrate was fixed at 100 V with an

Supported by the National Natural Science Foundation of China under contract Nos. 10275049 and 10435060.

*Corresponding author. E-mail: djfu@whu.edu.cn

Received date: 2005-12-26

80% duty factor. The input power to each pair of C targets was fixed at 12 kW, while the input power to the Ti targets was varied in order to prepare Ti-aC coatings with different Ti contents. Before deposition, a 30-min argon plasmas clean was carried out at 2 Pa gas pressure. The flow rate of Ar gas was kept constant at 80 sccm throughout the followed deposition process and the working pressure was 0.4 Pa. The mirror-polished cemented carbides and Si wafers were used as substrates and they were not heated during deposition; the chamber ambient temperature was lower than 100°C. The coating consists of a 15-min deposition of a pure Ti layer to improve the adhesion and a sequent 120-min deposition of Ti-aC composite coatings.

The surface morphologies of the Ti-aC coatings were measured on a SHIMADZU SPM-9500J3 atomic force microscope (AFM). Raman scattering measurements were carried out with an RM-1000 confocal Raman microspectrometer using an Ar-ion laser with an excitation wavelength of 514.5 nm. The Ti atomic content was determined by using an EDAX genesis 7000 EDS system operated at 25 kV. The hardness of the coatings was measured with a fully calibrated MTS Nano Indenter XP. An MS-T3000 Pin-on-disc tester was used for the friction and wear tests of the Ti-aC nanocomposite coatings, which slid in ambient air at 23^{o}C and relative humidity (RH) of 60%. Cemented carbide, Cu, Al-alloy, carbon steel, and stainless steel were used as mating materials in the wear measurements, where 5 N loads were applied on the samples.

3 Results and discussion

3.1 Surface morphology

Fig. 1 shows the surface morphology of the Ti-aC coatings. A sharpened pyramidal tip was used in the AFM measurement; and the lateral resolution is about 0.1 nm and the vertical resolution is about 0.02 nm. The AFM image shows a dense and homogeneous distribution of the coating surface. The surface roughness is markedly influenced by the Ti content. With the increase of Ti content, the root mean square roughness (rms) decreases from 7.31 to 2.55 nm. This is attributed to a combination of the smoothing effect of Ar ion bombardment and the disperse effect of Ti atom added to the coating, which results in the easy formation of amorphous carbon clusters and the prevention of relatively large clusters [7].

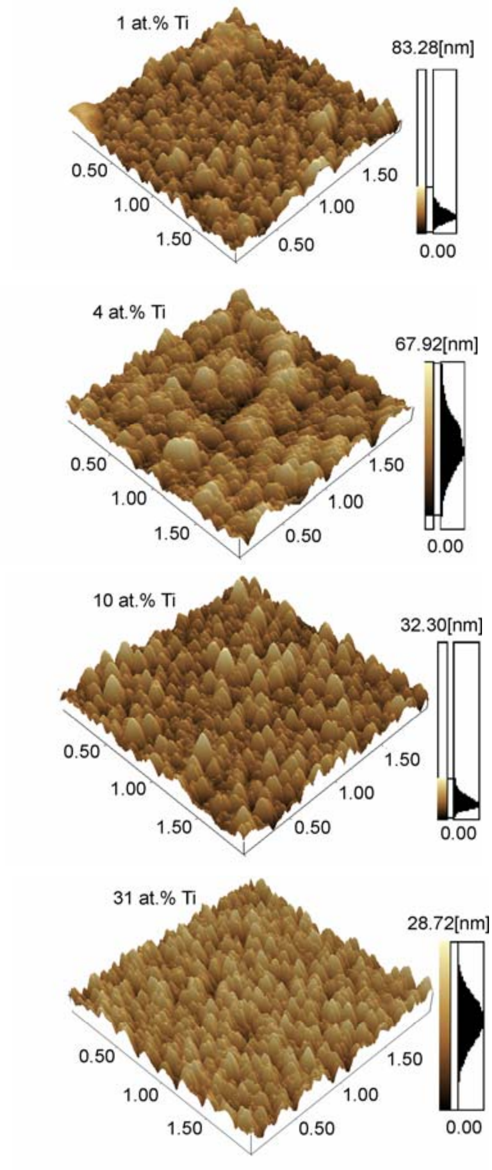

(a)

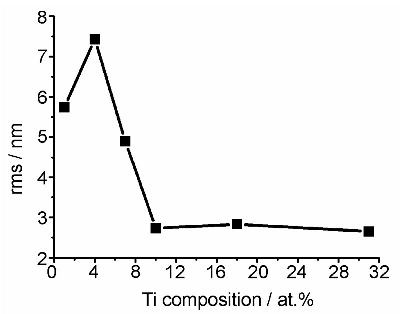

(b)

Fig.1 AFM images of Ti-aC coatings with various Ti content (a) and surface roughness in root-mean-square (rms) as a function of Ti content (b).

3.2 Raman spectra

Fig. 2 shows Raman spectra of Ti-aC coatings with different Ti content. It can be seen that when the Ti content is lower than 10 at.%, the coatings are typical diamond-like carbon. When the Ti content is higher than 10 at.%, a new peak, which can be assigned to TiC, appears in the range of 500-800 cm^{-1} and intensifies with increasing Ti content. The D and G peaks at lower Ti content are much sharper than those at higher Ti doping level, which is due to the small graphite crystallites present at lower Ti content, resulting in the activity of D peak. The broadening of D peak at higher Ti content is due to the increasing disorder in the carbon sheets.

To obtain more detailed information about the bonding structure in the films, Raman spectra were fitted by Gaussian curves, as shown in Fig. 3. With increasing Ti content the ratio of $I_{\mathrm{D}}/I_{\mathrm{G}}$ increases. This is believed to originate from increasing disorder of the coatings. In a theoretical study of Raman spectra for amorphous carbon, Beeman et al.[8] found that increased number of sp^3-bonded atomic sites in amorphous carbon results in a shift in the G-band position to a lower frequency. On the basis of this theory, in Fig. 3(b), the shift of G-band position to a lower frequency with increasing Ti content means that a high sp^3 fraction was formed, especially when Ti content is 10 at.%. This sample also demonstrates G and D peaks with larger FWHM (full width at half maximum), as shown in Fig. 3(c), confirming the above analysis.

3.3 Mechanical and tribological performance

The tribological performance is influenced significantly by the hardness of the coatings[9]. As shown in Fig. 4, with increasing Ti content, the hardness increases from 12 GPa at 1 at.% Ti to 27 GPa at 31 at.% Ti. When the Ti content is lower than 10 at.%, the higher hardness is mainly caused by the reduced size and the increased density of Ti nanograins, a typical result of grain boundary sliding[10]. When the Ti content is higher than 10 at.%, the increasing hardness results from a combination of the hard TiC phase, as revealed by the Raman spectra and the grain boundary sliding.

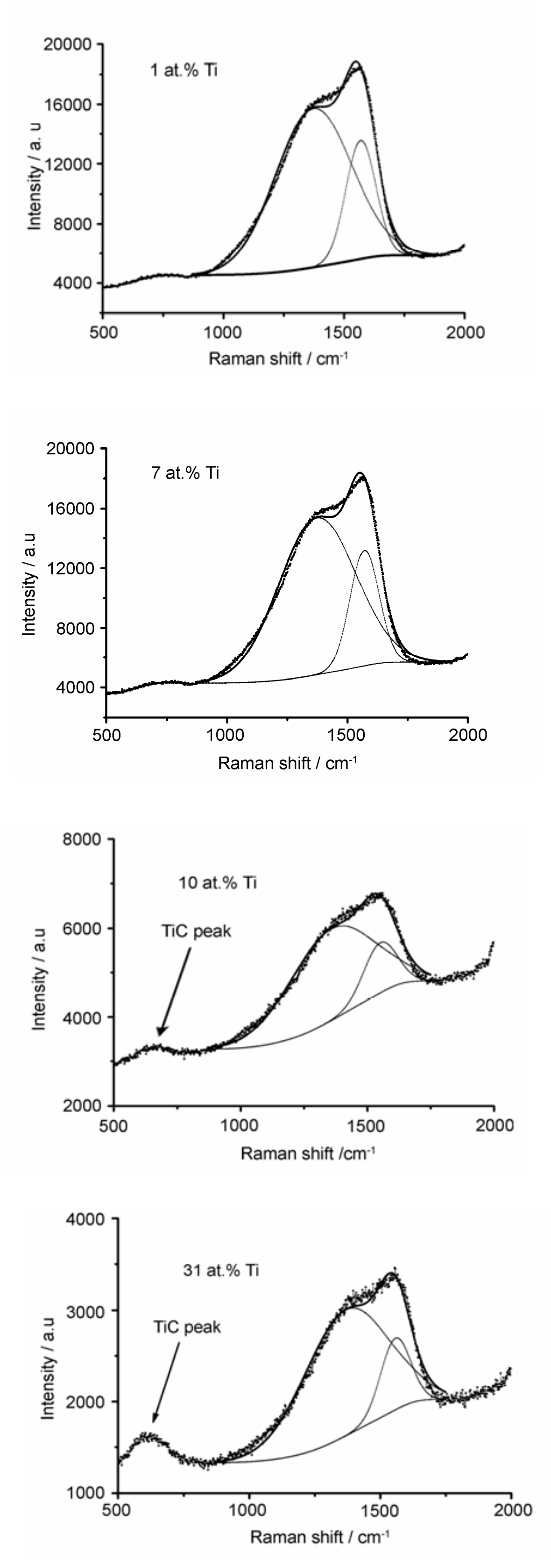

Fig.2 Raman spectra of Ti-aC coatings with different Ti content. The TiC peak appears when Ti content is higher than 10 at.%.

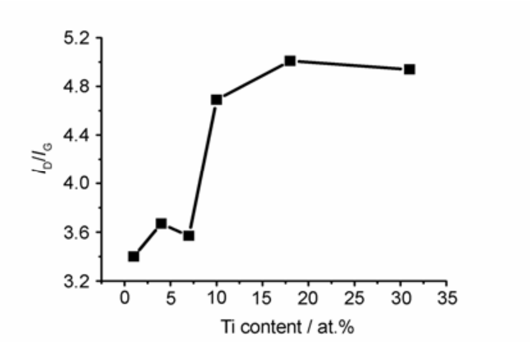

(a)

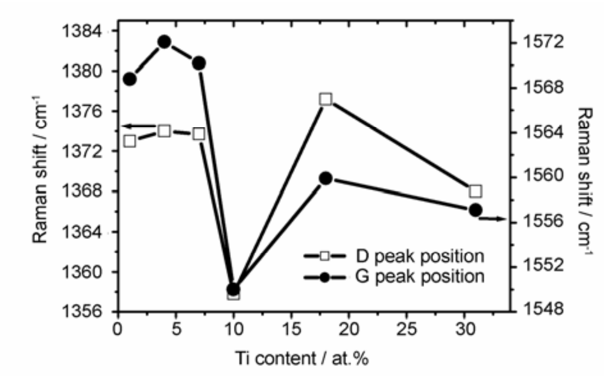

(b)

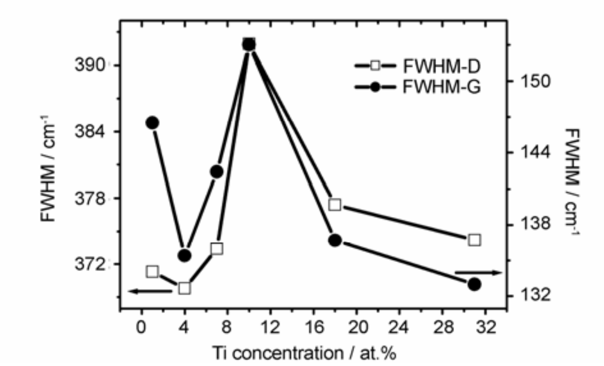

(c)

Fig.3 Fitted results of Raman spectra: (a), (b) I_D/I_G, peak position, and (c) FWHM as functions of Ti content.

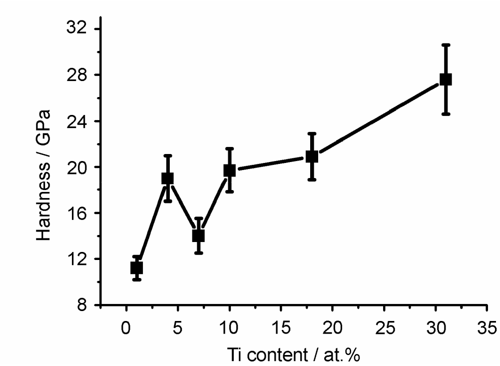

Fig.4 Hardness of the Ti-aC coatings as a function of Ti content.

Fig. 5(a) shows the friction coefficients of Ti-aC coatings prepared at a fixed bias of 100 V. The mating material for the measurement is cemented carbide. With increasing Ti content, the friction coefficient decreases first from 0.16 at below 4 at.% Ti to 0.07 at 4 at.% Ti, and then it increases up to 0.40 at 31 at.% Ti. This indicates that the Ti content plays an important role in the friction coefficients of the Ti-aC coatings when a hard mating material is used in the wear testing. Fig. 5(b) shows another trend of the friction coefficient with increasing Ti content when Al-alloy, Cu, carbon steel, and stainless steel are used as the mating material, respectively. It is clear, on the basis of Fig. 5(a) and (b) that in the case of a hard mating material, the wear debris from the coatings act as the lubricating substance, and the friction coefficients are mainly influenced by the coatings. In the case of soft Al-alloy, Cu, or steel as mating materials they are incorporated into the worn surface and act as the main lubricating element, hence, with increasing Ti content, the hardness of the coating increases, the wear rate of the coatings and the friction coefficient are reduced.

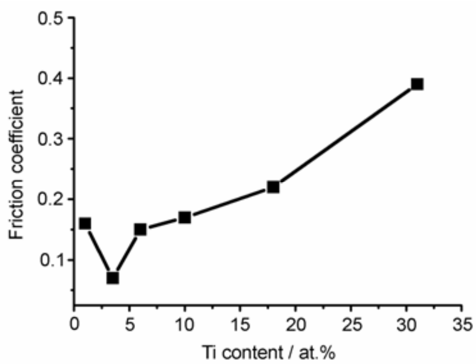

(a)

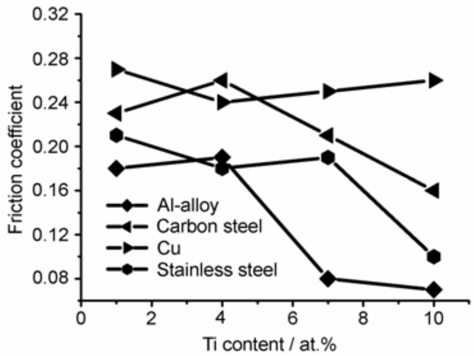

(b)

Fig.5 Friction coefficients of Ti-aC coatings with various mating materials.

4 Conclusion

Ti-aC nanocomposite coatings were synthesized by means of cathode-arc-assisted closed field middle-frequency unbalanced magnetron sputtering. Raman spectroscopic results showed that the structure of the coatings was significantly influenced by incorporating Ti in the coatings. The pin-on-disc test results showed that the coatings had different friction behavior when facing different mating materials. The mechanical and tribological performance of the Ti-aC coatings is evidently correlated with their chemical bonding structures.

References

1 Uglov V V, Kuleshov A K, Rusalsky D P, *et al*. Surf. Coat. Technol. 2000, **128-129**: 150-155.

2 Deng J, Braun M, Diamond and Related Materials. 1995, **4**: 936-943.

3 Daniel N, Fredrik S, Urban W, *et al*. Wear. 2003, **254**: 1084-1091.

4 Donnet C, Surf. Coat. Technol., 1998, **100-101**: 180.

5 Pauleau Y, Thiery F, Surf. Coat. Technol. 2004, **180-181**: 313.

6 Corbella C, Vives M, Pinyol A, *et al*. Surf. Coat. Technol. 2004, **177-178**: 409.

7 Bewilogua K, Wittorf R, Thomsen H, *et al*. Thin Solid Films, 2004, **447- 448**: 142-147.

8 Beeman D, Silverman J, Lynds R, *et al*. Phys. Rev. B, 1984, **30**: 870-875.

9 Kodali P, Walter K C, Nastasi M, Tribology International, 1997, **30**: 591-598.

10 Yang B, Huang Z H, Liu C S, *et al*. Jpn. J. Appl. Phys. 2005, **44**: L1022-L1025.